European Review for Medical and Pharmacological Sciences 2019; 23: 3951-3959

A study of regulatory effects of TLR4 and NF-κB on primary biliary cholangitis

Y. YU[1,2], M.-P. LI[2], B. XU[2], F. FAN[2], S.-F. LU[2], M. PAN[2], H.-S. WU[2]

[1]Jinan University, Guangzhou, Guangdong, China
[2]Department of Hepatobiliary Surgery, the First Affiliated Hospital of Guangxi University of Chinese Medicine, Nanning, Guangxi, China

Abstract. – OBJECTIVE: To investigate the regulatory effects of the Toll-like receptor 4 (TLR4) and the nuclear factor kappa-light-chain-enhancer of the activated B cells (NF-κB) on primary biliary cholangitis (PBC) and to analyze the possible mechanisms.

MATERIALS AND METHODS: A total of 24 C57BL/6 mice were randomly divided into M group (n=12, intraperitoneally injected with polyinosinic acid-polycytidine acid (Polyl:C) for 12 consecutive weeks, 2 times/week) and C group (n=12, intraperitoneally injected with the same volume of normal saline). After 12 weeks, the mice were sacrificed to collect liver tissues. Then, an enzyme-linked immunosorbent assay (ELISA) kit was used to detect the content of interleukin-6 (IL-6), IL-10, and tumor necrosis factor-alpha (TNF-α) in liver tissues. Hematoxylin-eosin (HE) staining assay was performed to observe the pathological changes of liver tissues, and measure the levels of alanine aminotransferase (ALT) and aspartate aminotransferase (AST) in peripheral blood of mice. Terminal deoxynucleotidyl transferase-mediated deoxyuridine triphosphate-biotin nick end-labeling (TUNEL) staining was applied to determine cell apoptosis in liver tissues. The relative messenger ribonucleic acid (mRNA) expression levels of TLR4 and NF-κB in liver tissues were detected by quantitative Polymerase Chain Reaction (qPCR). Western blotting was adopted to measure the protein expressions of TLR4, NF-κB, myeloid differentiation factor 88 (MyD88), B-cell lymphoma 2 (Bcl-2)/Bcl-2-associated X protein (Bax), and Caspase-3.

RESULTS: Compared with that in C group, the content of IL-6 and TNF-α in liver tissues in M group was significantly increased ($p<0.01$), but the level of IL-10 was statistically downregulated ($p<0.01$). According to HE staining, liver damage of mice in M group was evidently severer than that in C group, and the levels of ALT and AST in M group were significantly higher than those in C group ($p<0.01$). The amount of TUNEL-positive cells in liver tissues in M group was significantly greater than that in C group ($p<0.01$). The levels of TLR4 and NF-κB mRNA in liver tissues from M group were significantly elevated in comparison with the C group ($p<0.01$). Compared with those in C group, the expressions of TLR4, NF-κB, MyD88, and Caspase-3 proteins in M group showed statistical increases in liver tissues ($p<0.01$), whereas that of Bcl-2/Bax was significantly declined ($p<0.01$).

CONCLUSIONS: PBC activates the TLR4/MyD88/NF-κB signaling pathway, induces the release of inflammatory factors and produces a large number of apoptotic proteins, which results in liver damage and cell apoptosis in mice.

Key Words:
Primary biliary cholangitis, TLR4/MyD88/NF-ÐB signaling pathway, Apoptosis.

Introduction

Primary biliary cholangitis (PBC), as a common kind of chronic and progressive cholestatic liver disease in middle-aged and elderly women, may cause an overt increase of liver enzymes activities in patients, which therefore causes pathological changes of the liver[1-3]. The main clinical manifestations of PBC include fatigue and skin pruritus, but no evident symptoms are generally observed in patients in the early stage of the disease, and most patients are treated with elevated cholesterol[4]. Furthermore, the pathogenesis of PBC remains unclear. Various factors are considered involved in the occurrence of the disease. For example, genetic and environmental factors are able to result in the disordered immune response of the body, so that the bile ducts in the liver are attacked and destroyed by im-

Corresponding Author: Yuan Yu, MD; email: YuanYu2fw@163.com

mune cells. It accordingly gives rise to cholestasis and ultimately results in liver failure[5-6]. As to the treatment of PBC, ursodeoxycholic acid is currently used as a first-line drug, which is ubiquitously recommended. A study by Bajer et al[7] found that ursodeoxycholic acid significantly alleviated liver fibrosis in patients with PBC, significantly prolonged patient survival and improved the quality of life. It is proposed that the hepatocyte apoptosis is inhibited. The Toll-like receptor (TLR), which can participate in non-specific immunity of the body, is one of the important regulatory proteins in triggering an immune response in the body by recognizing antigens[8-9]. TLR4, a member of the TLR family, can be expressed in various cells including immune cells, endothelial cells, and epithelial cells. Kramer et al[10] manifested that TLR4 effectively regulated the transcription and translation of the inflammatory factors and exerted functions through further regulation of the expression of apoptotic proteins during inflammation regulation. Nuclear factor kappa-light-chain-enhancer of activated B cells (NF-κB) is a downstream target gene of TLR4, which can enter the nucleus and participate in the regulation of pro-inflammatory responses and immune responses once being activated[11]. Pei et al[12] discovered that NF-κB promoted the transformation of renal tubular epithelial cells, up-regulated the expressions of inflammatory factors, and further accelerated tubulointerstitial fibrosis. However, the exact function and mechanism of TLR4 and NF-κB in PBC remain elusive. In this study, the mouse models of PBC were established, and the regulatory effects of TLR4 and NF-κB on PBC and the corresponding mechanisms were therefore explored.

Materials and Methods

Experimental Animals and Grouping

A total of 24 female C57BL/6 mice aged 5-6 weeks old were purchased from the Experimental Animal Center, Guangzhou University of Chinese Medicine [Production License No. of experimental animals: SCXK (Guangdong) 2016-0004] (Guangzhou, Guangdong, China) and fed in SPF animal rooms at 50-60% humidity and 23±2°C, with 12 h of light per day and free access to food and water. The mice were acclimated to the breeding environment for 7 d. Then, they were randomly divided into the C group (n=12) and the M group (n=12). Mice in M group were intraperitoneally injected with polyinosinic acid-polycytidine acid (Poly I:C) for 12 consecutive weeks, twice a week, to establish mouse models of PBC, while those in C group were given an equal volume of normal saline as controls. The experimental protocol in this study was approved by the Laboratory Animal Ethics Committee of the First Affiliated Hospital of Guangxi University of Chinese Medicine. All operations involving animals were carried out in accordance with the relevant regulations of the NIH Guide for the Care and Use of Laboratory Animals.

Detection of the Content of Inflammatory Factors Via Enzyme-Linked Immunosorbent Assay (ELISA)

After 12 weeks of modeling, the mice in each group were euthanized, and the liver tissues were separated. Next, radioimmunoprecipitation assay (RIPA) lysis solution was added at a ratio of weight (g) : volume (mL) = 1 : 3 for quick homogenization, followed by centrifugation at 12,000 rpm and 4°C for 10 min. After that, the supernatant was collected and stored for later use. The content of the inflammatory factors [interleukin-6 (IL-6), IL-10 and tumor necrosis factor-alpha (TNF-α)] was detected using an ELISA kit (Wuhan Boster Biological Technology Co., Ltd., Wuhan, China) in strict accordance with its instructions. Firstly, the standard IL-6, IL-10, and TNF-α were diluted into solution with concentrations of 1,000, 500, 250, 125, 62.5, 31.3, 15.6 and 0 pg/mL, and a corresponding standard curve was plotted. Secondly, the biotin-labeled anti-mouse IL-6, IL-10, and TNF-α working fluid were prepared. Thirdly, the standard wells, sample wells, and blank control wells were set up. 100 μL corresponding solution was added to each well, the sealing with a plate sealing membrane was performed, and the plate was put in an incubator for 75 min of reaction at 37°C. Fourthly, the liquid in the plate was patted dry, and 100 μL biotin-labeled anti-mouse IL-6, IL-10, and TNF-α antibody were added, followed by sealing with the plate sealing membrane and 45 min of reaction at 37°C in the incubator. Then, the liquid in the plate was patted dry, and the washing buffer was added for washing. 100 μL avidin-peroxidase complex was added, sealed with the plate sealing membrane and placed in the incubator for 30 min of reaction at 37°C. Finally, the colored solution was added for color development at 37°C for 30 min, and then a stop buffer was added

to end the reaction. A microplate reader set at a wavelength of 450 nm was employed to measure the optical density (OD) value of each well, and a CurveExpert 1.6 software was utilized to analyze the content of inflammatory factors (IL-6, IL-10, and TNF-α) in liver tissues in each group.

Hematoxylin-Eosin (HE) Staining of Liver Tissues

The mice in each group were sacrificed after 12 weeks of modeling, followed by isolation of liver tissues. Then, phosphate-buffered saline (PBS) was prepared in advance and pre-cooled in a refrigerator. Next, the liver was washed with PBS, the blood was removed, and the adipose tissue and connective tissue on the surface of the liver were separated. After that, the liver tissues were fixed with 10% formalin overnight, and dehydrated with 95%, 90%, 75%, 60%, and 50% ethanol, respectively, and transparentized with xylene, followed by preparation of the paraffin sections (5 μm in thick). Thereafter, the sections were collected from each group, dewaxed with xylene, hydrated with gradient ethanol and stained with hematoxylin and eosin, respectively. After staining, the sections were dehydrated with 95%, 75%, and 50% ethanol, followed by transparency with xylene and mounted with neutral resin. Lastly, the morphological changes of liver tissues of mice were observed under bright field conditions using an inverted fluorescence microscope.

Determination of Alanine Aminotransferase (ALT) and Aspartate Aminotransferase (AST) Levels in Peripheral Blood

After 12 weeks of modeling, the peripheral blood was collected from each group of mice and centrifuged at 4°C and 3,000 rpm for 15 min, and the supernatant was taken. The plasma ALT and AST content were detected using mouse ALT and AST kits, strictly in accordance with the instructions of the kits (Nanjing Jiancheng Bioengineering Institute; Nanjing, Jiangsu, China).

Terminal Deoxynucleotidyl Transferase-Mediated Deoxyuridine Triphosphate-Biotin Nick End Labeling (TUNEL) Staining of Liver Tissues

After 12 weeks of modeling, the mice in each group were sacrificed, and liver tissues were separated. Next, the paraffin sections of liver tissues from each group were prepared, dewaxed, and washed with freshly-prepared PBS solution. A TUNEL staining kit (R&D Systems, Minneapolis, MN, USA) was used in strict accordance with its instructions. The sections were mounted with anti-fluorescence-quenched blocking buffer and observed using a confocal fluorescence microscope. The number of TUNEL-positive cells in liver tissues of each group of mice was calculated. TUNEL-positive cells, i.e., yellow-green fluorescence, indicated apoptosis.

Ribonucleic Acid (RNA) Extraction and Quantitative Polymerase Chain Reaction (qPCR)

Mice in each group were euthanized after 12 weeks of modeling, followed by the separation of liver tissues. Next, the tissues were added with TRIzol lysis solution at a ratio of 100 mg: 1 mL for lysis until no tissues were visible. Then, the tissues were centrifuged at 12,000 rpm and 4°C for 10 min. Total RNA extraction was carried out using RNA extraction kit (Vazyme Biotech Co., Ltd., Nanjing, Jiangsu, China) based on its instructions. Agarose gel and the microplate reader were used to determine the purity and the OD value of extracted RNA, respectively, followed by reverse transcription with a reverse transcription kit (Vazyme Biotech Co., Ltd., Nanjing, Jiangsu, China) and qPCR using a SYBR ExScript™ RT-PCR kit (TaKaRa, Otsu, Shiga, Japan). The primers synthesized by Tiangen Bios Co., Ltd. (Beijing, China) are shown in Table I, with glyceraldehyde-3-phosphate dehydrogenase (GAPDH) as an internal reference. The expression levels of corresponding genes were calculated by $2^{-\Delta\Delta Ct}$ method.

Table I. PCR primers.

MRNA	Sequence
TLR4	Forward primer: 5'-GCTTTCACCTCTGCCTTCAC-3' Reverse primer: 5'-CGAGGCTTTTCCATCCAATA-3'
NF-κB	Forward primer: 5'-GCTACACAGAGGCCATTGAA -3' Reverse primer: 5'-GTGGAGGAAGACGAGAGAGG-3'
GAPDH	Forward primer: 5'-CAGTGCCAGCCTCGTCTCAT -3' Reverse primer: 5'-AGGGCCATCCACAGTCTTC-3'

Measurement of Expression Levels of Related Proteins Through Western Blotting

After 12 weeks of modeling, the mice in each group were sacrificed, and the liver tissues were separated and added with RIPA lysis solution (Beyotime, Nanjing, Jiangsu, China) at a ratio of 100 mg: 1 mL. Then, 1% protease inhibitor and 1% phosphoric acid were added, respectively, followed by homogenization using an ultrasonic homogenizer. After extracting protein, a bicinchoninic acid (BCA) protein assay kit (Beyotime, Nanjing, Jiangsu, China) was used to detect the concentration of total protein in liver tissues of each group of mice, and a loading sample system with the same concentration was prepared, boiled at 95°C to inactivate the protein, and loaded in an equal volume. After electrophoresis, the membrane transfer and blocking, incubation with TLR4, NF-κB, myeloid differentiation factor 88 (MyD88), B-cell lymphoma 2 (Bcl-2), Bcl-2-associated X protein (Bax), Caspase-3 and GAPDH antibodies at 4°C were conducted overnight, followed by incubation with horseradish peroxidase (HRP)-conjugated secondary antibody at room temperature for 1 h. Thereafter, a luminescent solution was added for development. Lastly, bands were analyzed by the software, and the expression levels of the corresponding proteins in each group were calculated.

Statistical Analysis

All data in this study were expressed as mean ± standard deviation and processed and analyzed using SPSS 21.0 software (SPSS Inc., Armonk, NY, USA). A *t*-test was used for comparison between the two groups, and $p<0.05$ suggested that the difference was statistically significant.

Results

Content of Inflammatory Factors in Liver Tissues

The mice in each group were euthanized immediately after modeling, and the liver tissues were collected and subjected to homogenization. Then, the content of the inflammatory factors was

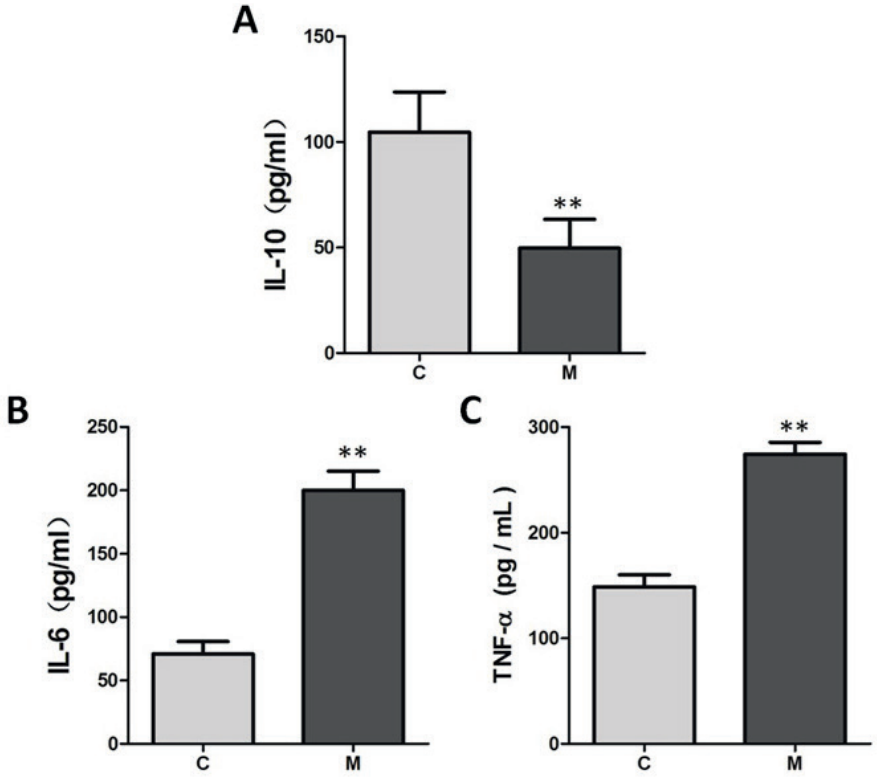

Figure 1. Inflammatory factors in liver tissues in each group detected using the ELISA kit. ***A,*** TL-10. ***B,*** IL-6. ***C,*** TNF-α. **$p<0.01$, compared with C group.

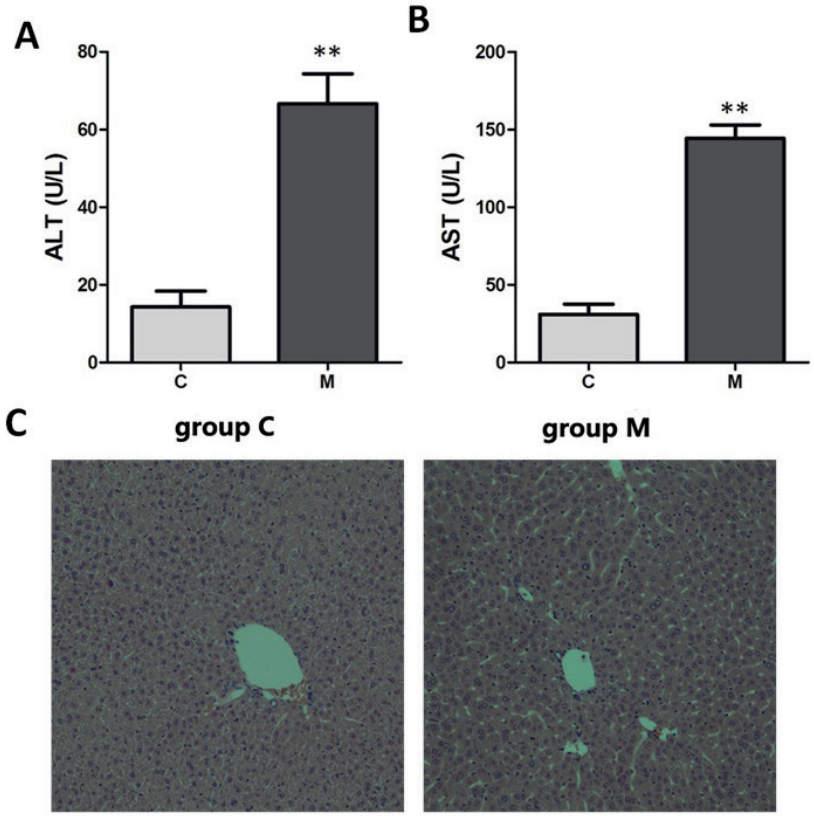

Figure 2. Liver damage in mice. ***A,*** ALT. ***B,*** AST. ***C,*** HE staining. The levels of ALT and AST in peripheral blood of mice in M group were significantly higher than those in C group. HE staining indicated that there was damage in liver tissues of M group.

measured, and the results (Figure 1) showed that the level of IL-10 in liver tissues of mice in M group was significantly lower than that in C group (p<0.01), whereas the contents of IL-6 and TNF-α were significantly elevated (p<0.01).

The Damage of Liver Tissue in Each Group of Mice

After modeling, the mice in each group were immediately sacrificed. The peripheral blood was taken to detect the levels of ALT and AST. HE staining was used to determine the pathological changes of liver tissues in each group. The results (Figure 2) manifested that the levels of both ALT and AST in peripheral blood of mice were elevated in the M group compared with those in the C group (p<0.01). The results of HE staining indicated that the liver tissue sections of C group had clear texture and compact cells, whereas evident hepatocyte degeneration, neutrophil infiltration, central venous, and hepatic sinus congestion and liver damage were shown in liver tissue sections of M group.

Apoptosis in Liver Tissues Determined through TUNEL Staining

The TUNEL staining kit was utilized to determine apoptosis in liver tissues in each group, and it was found that the amount of TUNEL-positive cells in liver tissues in M group was significantly increased than that in C group (p<0.01), indicating that the apoptosis in M group was severer than that in C group (Figure 3).

Relative Messenger RNA (mRNA) Expression Levels Measured Via qPCR

The TLR4 and NF-κB mRNA levels in liver tissues of mice were detected through qPCR. The results revealed that the relative expressions in M group were significantly increased in comparison with the C group (p<0.01) (Figure 4).

Expression of Related Proteins Detected through Western Blotting

Through Western blotting, the expressions of TLR4, NF-κB, and MyD88 proteins in liver tissues in M group were evidently higher than those

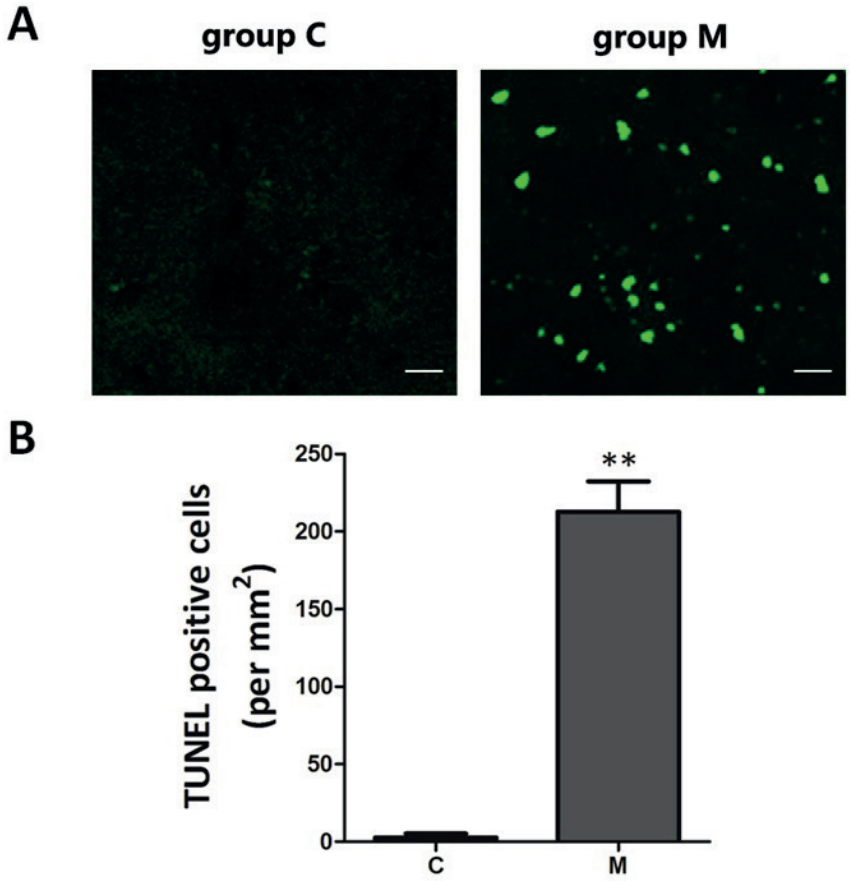

Figure 3. Apoptosis of TUNEL-stained hepatocytes. ***A,*** TUNEL staining microscopic image. ***B,*** Statistical chart, Bar=50 μm. The yellow-green fluorescence indicated TUNEL-positive cells. ***p*<0.01, compared with C group.

in the C group ($p<0.01$) (Figure 5). To further explore the mechanism of damage to liver tissue, Western blotting was further used to detect the expression levels of apoptosis-related proteins. The data showed that compared to the C group, overtly lowered Bcl-2/Bax level ($p<0.01$) and a distinctly elevated Caspase-3 level were observed in M group ($p<0.01$) (Figure 6).

Discussion

PBC is an immune-mediated cholestatic disease and a typical autoimmune disease. A research by Sun et al[13] found that both humoral and cellular immunity are involved in the pathogenesis of PBC. Endo et al[14] proved that a massive cluster of differentiation 8^+ ($CD8^+$) T cells infiltrates into the liver tissues of patients with PBC, especially in the hepatic duct area of the lesion, and that $CD8^+$T cells are an important cause of liver damage. TLRs, as important receptors mediating immune function and cell activation, are distributed in many immune cells (mainly in cells of the natural immune system). TLR-mediated signal activation leads to the increasing release of chemotactic factors and promotes the synthesis and secretion of inflammatory factors, whose overexpression may have a dreadful effect on the defense response of the body[15]. It was manifested that the expression of TLR4 in the inflammatory cell model was significantly increased, and it induced the evident increase in the expression of its downstream target NF-κB[16]. NF-κB acts as a nuclear transcription factor with multi-directional regulatory effects, it enters in the nucleus from the cytoplasm, and widely regulates various immune responses and stress responses. TLR4-mediated MyD88-dependent pathway affects the release of cytokines mainly by activating NF-κB[17].

In this study, the mouse models of PBC were established through intraperitoneal injection of

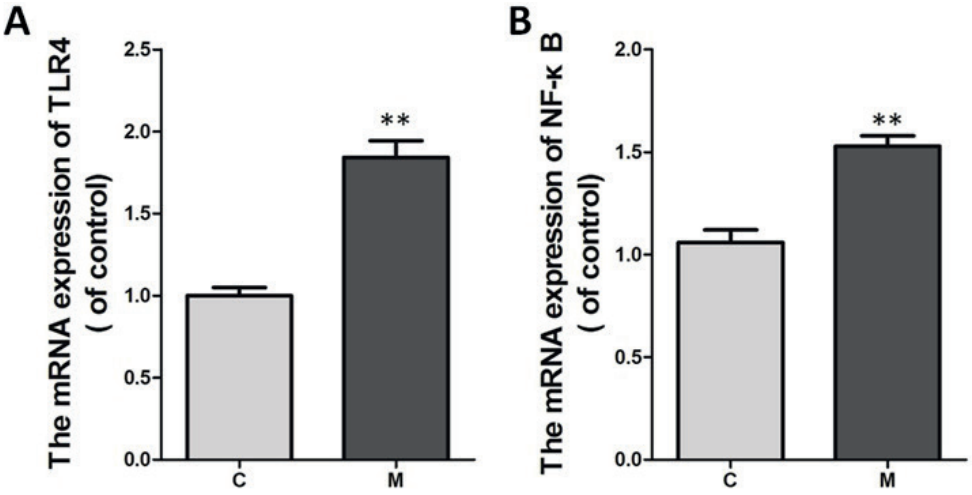

Figure 4. TLR4 and NF-κB mRNA levels in liver tissues of mice in each group measured via qPCR. **p<0.01, compared with C group.

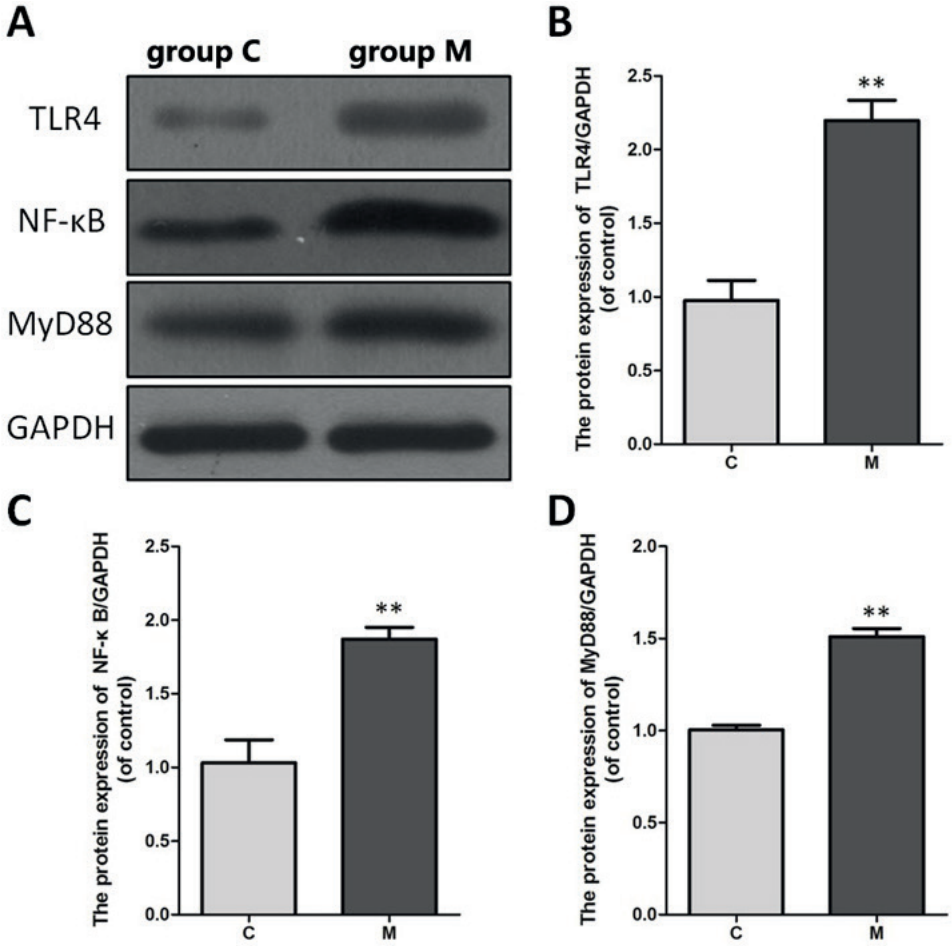

Figure 5. Expression levels of related proteins detected through Western blotting in each group of mice. ***A,*** Histogram. ***B,*** Expression level of TLR4. ***C,*** Expression level of NF-κB. ***D,*** Expression level of MyD88. **p<0.01, compared with C group.

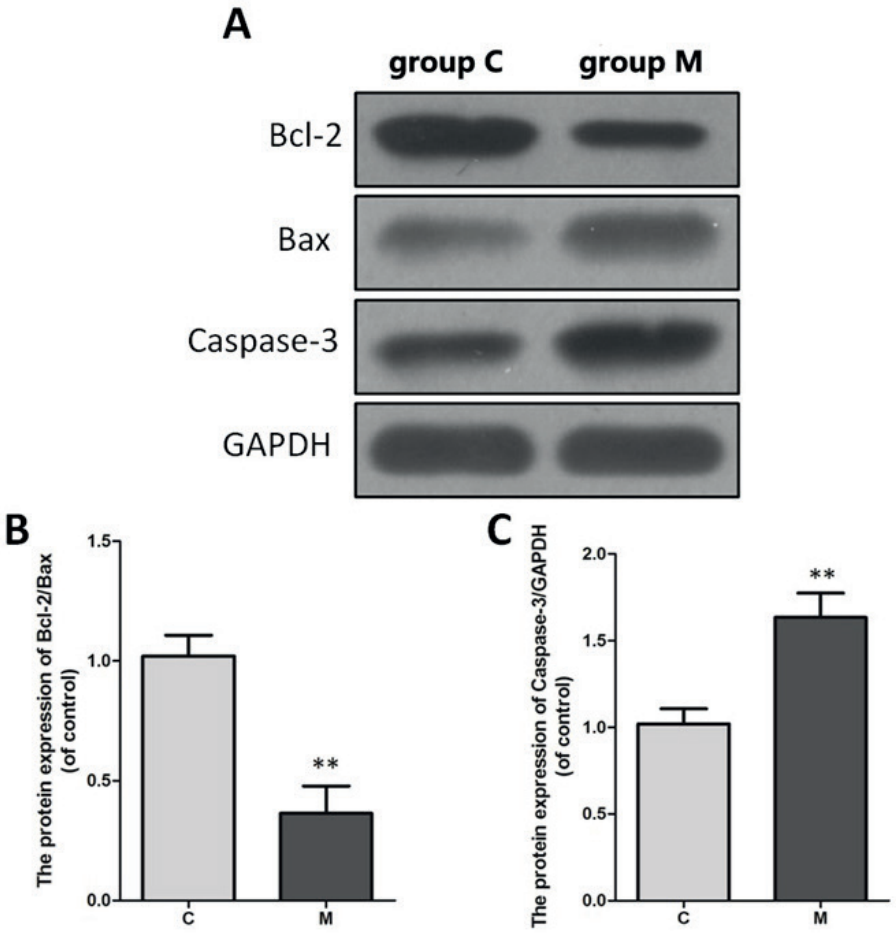

Figure 6. Expressions of apoptosis-related proteins in each group measured by Western blotting. ***A,*** Histogram. ***B,*** Expression level of Bcl-2/Bax. ***C,*** Expression level of Caspase-3. ***p<0.01, compared with C group.

Poly I:C to determine the regulatory effects of TLR4 and NF-κB on primary biliary cholangitis. This study found that mice in the M group presented evident liver tissue damage, with clearly-increased levels of inflammatory factor IL-6 and TNF-α and it significantly lowered the content of IL-10. Xiong et al[18] revealed that sepsis caused liver damage and increased the release of the inflammatory factors, and also discovered that the production of the inflammatory factors in liver tissues can be effectively reduced by relieving the symptoms of sepsis. Our data showed that the mRNA and protein levels of TLR4 and NF-κB were significantly higher in PBC mice than in normal mice. Previous evidence indicated that the TLR pathway-mediated inflammatory response played an important role in the pathogenesis of PBC and increased the release and activation of TLR, as well as the expressions of various downstream kinase via the MyD88-dependent pathway or TRIF[19]. Basically, NF-κB binds to the inhibitor of NF-κB (IκB) in a physiological manner. However, the stimulation of pathological factors leads to the degradation of IκB, and thereby further activated NF-κB. It then enters in the nucleus and regulates the transcription and translation of relevant downstream inflammatory factors and cytokines and promotes their expressions[20]. We found that the number of TUNEL-positive cells in liver tissues of PBC mice was significantly increased, and it is hypotesized as the partial reason for the liver damage. Recent findings showed the possibility of intervention with TLR4/NF-κB and anti-inflammatory and anti-oxidative therapy as a new target to reverse the left ventricular remodeling[21]. In this regard, our data offers academic support for the future treatment of primary biliary cholangitis by targeting TLR4/NF-κB.

Conclusions

We observed that PBC promotes the release of the inflammatory factors by activating the TLR4/MyD88/NF-κB signaling pathway and results in liver cell apoptosis and tissue damage, suggesting that the inhibition of TLR4/NF-κB may alleviate PBC.

Conflict of interest

The authors declare no conflicts of interest.

Acknowledgements

This paper was supported the by National Natural Science Foundation of China (No. 81760870); Guangxi Natural Science Foundation (No. 2017GXNSFAA198120).

References

1) To U, Silveira M. Overlap syndrome of autoimmune hepatitis and primary biliary cholangitis. Clin Liver Dis 2018; 22: 603-611.
2) Chascsa DM, Lindor KD. Antimitochondrial antibody-negative primary biliary cholangitis: is it really the same disease? Clin Liver Dis 2018; 22: 589-601.
3) Song Y, Yang H, Jiang K, Wang BM, Lin R. MiR-181a regulates Th17 cells distribution via up-regulated BCL-2 in primary biliary cholangitis. Int Immunopharmacol 2018; 64: 386-393.
4) Lleo A, Colapietro F. Changes in the epidemiology of primary biliary cholangitis. Clin Liver Dis 2018; 22: 429-441.
5) Wunsch E, Raszeja-Wyszomirska J, Barbier O, Milkiewicz M, Krawczyk M, Milkiewicz P. Effect of S-adenosyl-L-methionine on liver biochemistry and quality of life in patients with primary biliary cholangitis treated with ursodeoxycholic acid. A prospective, open label pilot study. J Gastrointestin Liver Dis 2018; 27: 273-279.
6) Kremer AE, Le Cleac'h A, Lemoinne S, Wolf K, De Chaisemartin L, Chollet-Martin S. Antipruritic effect of bezafibrate and serum autotaxin measures in patients with primary biliary cholangitis. Gut 2018. pii: gutjnl-2018-317426.
7) Bajer L, Wohl P, Drastich P. PSC-IBD: specific phenotype of inflammatory bowel disease associated with primary sclerosing cholangitis. Vnitr Lek 2018; 64: 659-664.
8) Michels KR, Lukacs NW, Fonseca W. TLR activation and allergic disease: early life microbiome and treatment. Curr Allergy Asthma Rep 2018; 18: 61.
9) Balka KR, De Nardo D. Understanding early TLR signaling through the Myddosome. J Leukoc Biol 2019; 105: 339-351.
10) Kramer B, Franca LM, Zhang Y, Paes AMA, Gerdes AM. Western diet triggers Toll-like receptor 4 (TLR4) signaling-induced endothelial dysfunction in female Wistar rats. Am J Physiol Heart Circ Physiol 2018; 315: H1735-H1747.
11) Cao C, Yin C, Chai Y, Jin H, Wang L, Shou S. Ulinastatin mediates suppression of regulatory T cells through TLR4/NF-κB signaling pathway in murine sepsis. Int Immunopharmacol 2018; 64: 411-423.
12) Pei W, Zou Y, Wang W, Wei L, Zhao Y, Li L. Tizanidine exerts anti-nociceptive effects in spared nerve injury model of neuropathic pain through inhibition of TLR4/NF-κB pathway. Int J Mol Med 2018; 42: 3209-3219.
13) Sun Y, Shao C, Qu H, Zuo G, Jing T, Wan T, Ji S. Primary biliary cholangitis associated with drug-induced liver injury and alcoholic liver fibrosis: a case report. Medicine 2018; 97. e12395.
14) Endo S, Watanabe Y, Abe Y, Shinkawa T, Tamiya S, Nishihara K, Nakano T. Hepatic inflammatory pseudotumor associated with primary biliary cholangitis and elevated alpha-fetoprotein lectin 3 fraction mimicking hepatocellular carcinoma. Surg Case Rep 2018; 4: 114.
15) El-Abhar H, Abd El Fattah MA, Wadie W, El-Tanbouly DM. Cilostazol disrupts TLR-4, Akt/GSK-3β/CREB, and IL-6/JAK-2/STAT-3/SOCS-3 crosstalk in a rat model of Huntington's disease. PLoS One 2018; 13: e0203837.
16) Buchrieser J, Oliva-Martin MJ, Moore MD, Long JCD, Cowley SA, Perez-Simón JA, James W, Venero JL. RIPK1 is a critical modulator of both tonic and TLR-responsive inflammatory and cell death pathways in human macrophage differentiation. Cell Death Dis 2018; 9: 973.
17) Liu L, Pang XL, Shang WJ, Xie HC, Wang JX, Feng GW. Over-expressed microRNA-181a reduces glomerular sclerosis and renal tubular epithelial injury in rats with chronic kidney disease via down-regulation of the TLR/NF-κB pathway by binding to CRY1. Mol Med 2018; 24: 49.
18) Xiong CQ, Zhou HC, Wu J, Guo NZ. The Protective effects and the involved mechanisms of Tanshinone IIA on sepsis-induced brain damage in mice. Inflammation 2019; 42: 354-364.
19) Xuan H, Yuan W, Chang H, Liu M, Hu F. Anti-inflammatory effects of Chinese propolis in lipopolysaccharide-stimulated human umbilical vein endothelial cells by suppressing autophagy and MAPK/NF-κB signaling pathway. Inflammopharmacology 2018. doi: 10.1007/s10787-018-0533-6 [Epub ahead of print].
20) Ju M, Liu B, He H, Gu Z, Liu Y, Su Y, Zhu D, Cang J, Luo Z. MicroRNA-27a alleviates LPS-induced acute lung injury in mice via inhibiting inflammation and apoptosis through modulating TLR4/MyD88/NF-κB pathway. Cell Cycle 2018; 17: 2001-2018.
21) Jiang H, Qu P, Wang JW, Li GH, Wang HY. Effect of NF-kappaB inhibitor on Toll-like receptor 4 expression in left ventricular myocardium in two-kidney-one-clip hypertensive rats. Eur Rev Med Pharmacol Sci 2018; 22: 3224-3233.